ACS APPLIED MATERIALS & INTERFACES

Article

Integration of Biofuel Cell-based Self-Powered Biosensing and Homogeneous Electrochemical Strategy for Ultrasensitive and Easy-to-Use Bioassays of MicroRNA

Panpan Gai, Chengcheng Gu, Ting Hou, and Feng Li

ACS Appl. Mater. Interfaces, **Just Accepted Manuscript** • DOI: 10.1021/acsami.8b01001 • Publication Date (Web): 02 Mar 2018

ACS Publications

ACS Applied Materials & Interfaces is published by the American Chemical Society.
1155 Sixteenth Street N.W., Washington, DC 20036

Integration of Biofuel Cell-based Self-Powered Biosensing and Homogeneous Electrochemical Strategy for Ultrasensitive and Easy-to-Use Bioassays of MicroRNA

Panpan Gai, Chengcheng Gu, Ting Hou and Feng Li*

College of Chemistry and Pharmaceutical Sciences, Qingdao Agricultural University, Qingdao 266109, P. R. China.

* Corresponding author. Tel/Fax: 86-532-86080855

E-mail: lifeng@qust.edu.cn

ABSTRACT

Biofuel cell (BFC)-based self-powered biosensors have attracted substantial attentions due to their unique merits of no need for power sources (only two electrodes needed). More importantly, in case it can also work in homogeneous system, more efficient and easy-to-use bioassays could come true. Thus, herein, we proposed, a novel homogeneous self-powered biosensing strategy *via* integration of BFC and homogeneous electrochemical method, which was further utilized for ultrasensitive microRNA (miRNA) detection. To construct such an assay protocol, the cathodic electron acceptor $[Fe(CN)_6]^{3-}$ was entrapped in the pores of positively charged mesoporous silica nanoparticles and capped by the bio-gate DNAs. Once the target miRNA existed, it would trigger the controlled release of $[Fe(CN)_6]^{3-}$, leading to dramatical increase of the open circuit voltage. Consequently, the "signal-on" homogeneous self-powered biosensor for ultrasensitive miRNA assay was realized. Encouragingly, the limit of detection for miRNA-21 assay was down to 2.7 aM (S/N=3), obviously superior to other analogous reported approaches. This work not only provides an ingenious idea to construct the ultrasensitive and easy-to-use bioassays of miRNA, but also exhibits a successful prototype of portable and on-site biomedical sensor.

KEYWORDS

Biofuel cell; Self-powered biosensing; Homogeneous electrochemical method; MicroRNA assay; Cathodic electron acceptor

INTRODUCTION

Biofuel cells (BFCs) have recently undergone rapid development because of their ability to provide sustainable energy from renewable fuel sources under mild conditions.[1-5] Among them, BFC-based self-powered biosensors [6-7] have become a research focus due to the unique characteristics of no need for external power sources, simple fabrication process, miniature size, good anti-interference ability, and low cost. And they have been widely applied in environmental monitoring,[8-9] molecular diagnostics,[10-13] immunoassay,[14-15] cytosensing[16-17] and drug release,[18-20] *etc*. To date, the design principles of self-powered sensing strategies are mainly based on substrate effect, inhibition effect, blocking effect, enzyme activity, *etc*.,[7, 21-23] most of which rely on the biorecognition of biofuel by enzymes in solid-phase or DNA probes immobilized on the anode or cathode. However, the immobilization of biorecognition probes generally required particular experiment conditions and complicated experimental process, and the inappropriate immobilization would result in lower or even no signal response.[24-25] By contrast, homogeneous electrochemical assays can directly detect target molecules in homogeneous solution without any bioprobes immobilization, which could greatly benifit the construction of rapid, cost-effective, and easy-to-use bioassays. Hence, it could be significantly meaningful to develop the novel sensing strategy intergration of BFC and homogeneous electrochemical detection.

To demonstrate the proof-of-concept, we take microRNAs (miRNA-21) assay as the example. As we know, the abnormal expression of miRNAs in malignant tissues can function either as oncogenes or tumor suppressors during cancer initiation, progression, and metastasis.[26] To date, great efforts have been made for miRNA assays, including Northern blotting,[27] microarray hybridization[28], quantitative reverse transcription polymerase chain reaction (qRT-PCR),[29] colorimetric,[30] fluorescent,[31-34] surface enhanced Raman scattering (SERS),[35] intracellular imaging,[36-37] magnetic relaxation switch (MRS)[38] and electrochemical methods.[39-41] However, the shortcomings of complicated configuration, relatively low sensitivity, and high cost are incompatible with the easy-to-use requirements. Recently, the self-powered heterogeneous biosensing of miRNAs has been firstly reported,[42] which still required complex fabrications. As a consequence, on the basis of the unique features of both BFC and the DNA-based homogeneous electrochemistry, more efficient and easy-to-use BFC-based self-powered homogeneous biosensing strategy is considerable but underexplored.

Inspired by our previous work based on homogeneous electrochemical strategy for miRNA detection,[43-45] herein, we proposed a novel BFC-based self-powered homogeneous biosensing strategy for ultrasensitive miRNA bioassay. In details, the one-compartment biosensor was composed of the cathode based on DNA functionalized positively charged mesoporous silica nanoparticles (PMSN) and the anode based on glucose oxidase/carbon nanotube/gold nanoparticles (GOx/CNT/AuNPs). Intially, the electron acceptor, *i.e.* $[Fe(CN)_6]^{3-}$ was entrapped in the pores of positively charged PMSN and capped by the bio-gate DNA (denoted as csDNA) completely complementary to the target miRNA. In the absence of miRNA, $[Fe(CN)_6]^{3-}$ was encapsulated in the pores of PMSN, a low open circuit voltage (E^{OCV}) was observed (Scheme 1A). Once the target miRNA existed, it could hybridize with the capped csDNA to form the rigid DNA–RNA hetero-duplex structure, which would further separate from the PMSN surface due to the significantly decreased adhesion, and then the bio-gate on the csDNA-capped PMSN was efficiently opened,[46] resulting in the controlled release of the entrapped $[Fe(CN)_6]^{3-}$. As such, due to the high catalytic ability of the anode on glucose oxidation, the electrons produced by the anode were transferred to the cathode, leading to the reduction of $[Fe(CN)_6]^{3-}$, and the corresponding E^{OCV} dramatically increased (Scheme 1B). Overall, the ultrasensitive detection of miRNA was realized based on the as-proposed proof-of-concept and target-triggered strategy. This effective biosensing strategy could integrate the ingenious merits of self-powered BFC sensors and homogeneous electrochemistry, which demonstrates great potential as a versatile tool in bioassay and early diagnosis of cancers.

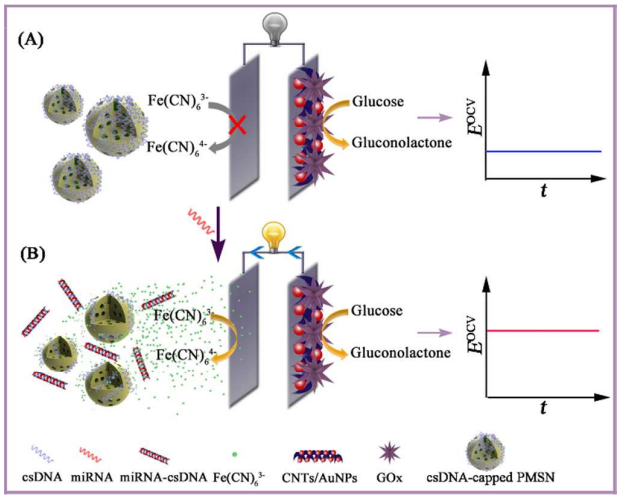

Scheme 1. Schematic illustration of the principle of the homogeneous self-powered biosensor in

the absence (A) and presence (B) of miRNA.

EXPERIMENTAL SECTION

Materials and Reagents. HPLC-purified miRNA and HPLC-purified DNA oligonucleotides were obtained from Shanghai Sangon Biotechnology Co., Ltd. (Shanghai, China). Glucose oxidase (GOx) from *Aspergillus niger* (EC 1.1.3.4, 158.9 units mg^{-1}), 1-ethyl-3-(3-dimethyl-aminopropyl) carbodiimide hydrochloride (EDC), *N*-hydroxysuccinimide (NHS), tetraethoxysilane (TEOS), cetyltrimethylammonium bromide (CTAB), and poly(diallyldimethylammonium chloride) (PDDA, 20%, w/w in water, M_W = 200 000-350 000), were all purchased from Sigma-Aldrich (St. Louis, MO, USA). Chloroauric acid ($HAuCl_4 \cdot 4H_2O$) and tris(hydroxymethyl)aminomethane (Tris) were obtained from Shanghai Chemical Reagent Co. Ltd. (Shanghai, China). Before use, the miRNA and csDNAs were diluted with 100 mM Tris-HCl (pH 7.4) to give the stock solutions. The carboxyl-functionalized AuNPs were prepared according to the literature by adding a sodium citrate solution to a boiling $HAuCl_4$ solution.[47] Ultrapure water (resistivity > 18.2 MΩ cm at 25°C) was obtained from a Milli-Q water purification system (Millipore Corp., Bedford, MA, USA). Diethyl pyrocarbonate (DEPC)-treated ultrapure water was used in all experiments. All reagents were of analytical grade and used without further purification. The sequences of the oligonucleotides are listed in Table S1 (in Supporting Information).

Apparatus. Electrochemical impedance spectroscopy (EIS) was carried on an Autolab PGSTAT 302N electrochemical analyzer (Metrohm Autolab, The Netherlands) within a frequency range of 0.1 to 100 kHz in 2.5 mM $[Fe(CN)_6]^{3-}/[Fe(CN)_6]^{4-}$ probe solution. Cyclic voltammetric (CV), linear sweep voltammetric (LSV), and the open circuit voltage E^{OCV} of BFC measurements were performed on a CHI 660E electrochemical workstation (Shanghai CH Instrument Co., China) using a three-electrode system: the fabricated anode or cathode as the working electrode, a Pt wire as the counter electrode, and an Ag/AgCl as the reference electrode. The open circuit voltage E^{OCV} of BFC was measured by connecting the anode and the cathode placed in the electrolytic cell. All experiments were carried out at room temperature (25 ± 1°C).

Loading of $[Fe(CN)_6]^{3-}$ into csDNA-Capped PMSN. Firstly, positively charged mesoporous silica nanoparticles (PMSN) was prepared and characterized by transmission electron microscopy and N_2 adsorption−desorption isotherm, described in our previous report in details.[48] Next, 10.0 mg of the above prepared PMSN was suspended into 1.0 mL of 1.0 M $[Fe(CN)_6]^{3-}$ solution, and

then the mixture was gently shaken at room temperature overnight. During this process, $[Fe(CN)_6]^{3-}$ entered the pores of the PMSN *via* diffusion. Subsequently, 10 μL of 1 nM csDNA was incubated with PMSN at room temperature for 4 h under gentle stirring. As a result, the csDNA was attached onto the PMSN *via* electrostatic interaction and formed the bio-gates. The mixture was then centrifuged (3,000 rpm, 2 min) and washed at least three times to remove any unloaded $[Fe(CN)_6]^{3-}$. Finally, the obtained csDNA-capped PMSN loaded with $[Fe(CN)_6]^{3-}$ was resuspended into 1.0 mL Tris-HCl buffer (pH 7.4, containing 0.1 M NaCl). As a control, random DNA sequence (rDNA)-Capped PMSN were prepared in a similar process except that rDNA was used as the bio-gate instead of csDNA.

Homogeneous Electrochemical Measurement on BFC Cathode. Indium tin oxide (ITO) electrodes were used as the substrate electrodes, and $[Fe(CN)_6]^{3-}$ acted as the electron acceptor of the BFC cathode. For the control experiment, 50 μL of csDNA-capped PMSN was added to 5 mL of Tris-HCl buffer (pH 7.4, 100 mM), and the electrochemical signals of $[Fe(CN)_6]^{3-}$ were detected by CV and LSV experiments with the potential ranging from −0.2 to 0.6 V (*vs* Ag/AgCl). Whereas, in the case of the target being present, 5 μL of miRNA-21 with different concentrations was first incubated with 50 μL of csDNA-capped PMSN at 37 °C for 2 h. The resulting mixture was then added to 5 mL of Tris-HCl buffer (pH 7.4, 100 mM) and mixed well. Finally, the electrochemical response of $[Fe(CN)_6]^{3-}$ was obtained through the CV and LSV measurements.

Preparation of GOx/CNT/AuNPs/ITO Anode. 8.0 mg of CNT was dispersed in 1% PDDA (4.0 mL) and then sonicated for 30 min to form a homogeneous suspension of positively charged CNT/PDDA. Residual PDDA polymer was removed by centrifugation (15000 rpm, 10 min), and the obtained precipitate was washed with ultrapure water at least three times, following which, the purified CNT/PDDA was mixed with 3.0 mL of AuNPs (10 nM) and then the mixture was gently shaken at room temperature overnight. Then excessive AuNPs were removed by centrifugation (8000 rpm, 10 min) and the CNT/AuNPs hybrid precipitate was resuspended in ultrapure water to bring the concentration to 1 mg mL^{-1}. The GOx/CNT/AuNPs/ITO anode was prepared by first casting 50μL of the as-prepared CNT/AuNPs suspension on the surface of the ITO substrate electrode. Then, the CNT/AuNPs electrode was dried at 37°C for 2 h and immersed in a solution containing 1 mg mL^{-1} EDC and 1 mg mL^{-1} NHS for 30 min. After rinsing with ultrapure water to remove excess EDC and NHS, the activated electrodes were incubated in 500 μL of GOx (10 mg

mL^{-1}) solution at 4°C for 12 h. The electrodes were rinsed repeatedly with water and soaked in PBS (pH 7.4) under stirring to remove any loose materials. The electrodes were stored at 4°C when not in use.

Homogeneous Self-Powered Biosensing for miRNA. A membrane-less glucose/$[Fe(CN)_6]^{3-}$ BFC was constructed by using the modified anode and ITO cathode and operated at room temperature. The supporting electrolyte was 5 mL of 100 mM Tris-HCl (pH 7.4) containing 5 mM of glucose. In the absence of the target miRNA, 50 μL of csDNA-capped PMSN was added to the supporting electrolyte, and the open circuit voltage of the BFC was measured, which was denoted as E_0^{OCV}. In the presence of the target miRNA, 5 μL miRNA-21 with different concentrations or the serum samples were incubated with 50 μL of csDNA-capped PMSN at 37 °C for 2 h, then the mixture was added to the supporting electrolyte, and the E^{OCV} of the BFC was measured again.

RESULTS AND DISCUSSION

Construction of csDNA-Capped PMSN. According to the aforementioned design principle, it can be deduced that the assembly of the csDNA-capped PMSN and the liberation of csDNA are the decisive protocol. As illustrated in Figure 1A, PMSN was obtained *via* the functionalization of MSN with positively charged polymer PDDA, and then $[Fe(CN)_6]^{3-}$ could diffuse into the pores of PMSN. Subsequently, the negatively charged csDNA, which acted as a gatekeeper, was attached onto PMSN surface *via* electrostatic interaction. In this case, $[Fe(CN)_6]^{3-}$ was entrapped in the pores of PMSN. To confirm this feasibility, first, the morphology and pore diameter of MSN was characterized by TEM and BET measurement. From Figure 1B and 1C, MSN exhibited the uniform structures with an everage diameter of 100~120 nm. Meanwhile, it also showed excellent BET surface area of 423 $m^2\ g^{-1}$ and well-defined pore size are of 2.5 nm, which guaranteed the efficient load of $[Fe(CN)_6]^{3-}$. Furthermore, the TEM images strongly identified the assembly and liberation of the bio-gate. As shown in Figure 1D and 1E, csDNA-capped PMSN showed much rougher surface and more blurred pores than those of MSN, indicating that csDNA has been successfully adhered onto the PMSN. After incubated with the target miRNA, the pore outline of MSN became relatively clear due to the liberation of the rigid DNA–RNA hetero-duplex structure. In addition, the zeta potential analysis was also carried out to confirm this protocol. The zeta-potential value of MSN was switched from -5.23 mV to +41.6 mV after the PDDA treatment,

benefited from the adsorption of the positively charged PDDA. Just as expected, the zeta-potential value drastically decreased to -50.3 mV, implying the adsorption of negatively charged csDNA on PMSN, and it could recover to a certain extent due to the detachment of DNA–RNA hetero-duplex. All the above results verified the successful fabrication of the csDNA-capped PMSN and the ability of target-induced csDNA liberation.

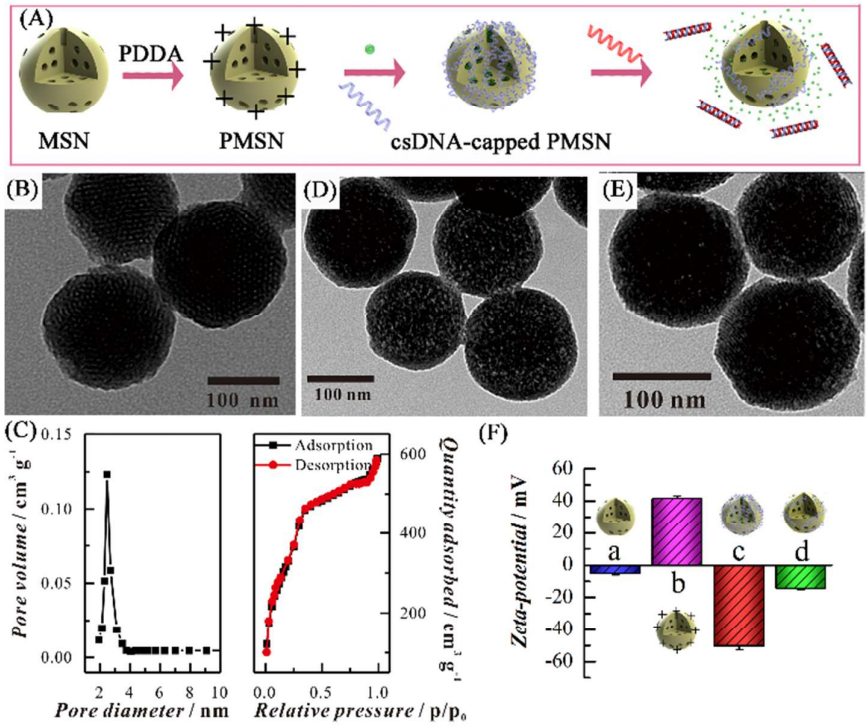

Figure 1. (A) Schematic illustration of the construction of csDNA-capped PMSN and the target-induced csDNA detachment; TEM images of MSN (B), csDNA-capped PMSN (D), and csDNA-capped PMSN incubated with miRNA (E); (C) Pore size distribution and N_2 adsorption-desorption isotherm of MSN; (F) Zeta potential of MSN(a), PMSN(b), csDNA-capped PMSN(c), and csDNA-capped PMSN incubated with miRNA (d).

To judge whether the target miRNA could trigger the controlled release of $[Fe(CN)_6]^{3-}$, CV and LSV measurements were performed to investigate the variation of the cathodic signal with different miRNA concentrations. As illustrated in Figure 2A, in the absence of miRNA-21, a pair of smaller redox peaks for $[Fe(CN)_6]^{3-/4-}$ were observed. And then the peak current gradually increased with the miRNA-21 concentration from 0.01 to 1000 fM, which can be attributed to that miRNA with higher concentration would hybridize with more csDNA, thus leading to a larger

amount of bio-gates opened, as well as more entrapped $[Fe(CN)_6]^{3-}$ released. Similarly, the LSV results (Figure 2B) also confirmed the release process controlled by the target miRNA because the cathodic peak current obviously increased when the DNA-RNA rigid double helix structure formed (curve b). In addition, to demonstrate the signal indeed originated from the specific Watson-Crick interaction between bases, not the leak of $[Fe(CN)_6]^{3-}$, the control experiments based on random DNA sequence (rDNA) capped PMSN were measured. As shown in Figure S1, the CV signals almost unchanged even the concentration of miRNA-21 was up to 1000 fM. All the above results confirmed the release process of the entrapped $[Fe(CN)_6]^{3-}$ which further illustrated the feasibility for assembling the BFC-based homogeneous self-powered biosensor.

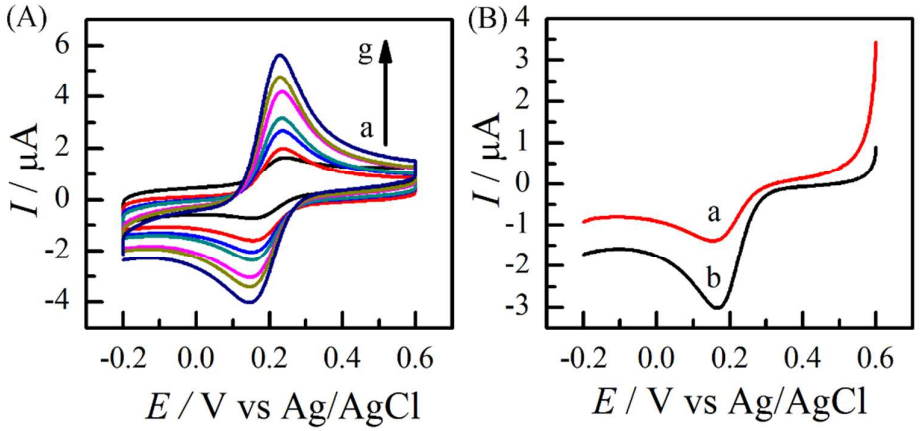

Figure 2. (A) CVs responses of $[Fe(CN)_6]^{3-}$ at the cathode in the presence of miRNA-21 with different concentrations (from a to g: 0, 0.1 , 0.5, 1.0, 10 , 100, and 1000 fM); (B) LSV of $[Fe(CN)_6]^{3-}$ at the cathode before (a) and after (b) the treatment with 10 fM miRNA-21. All CVs and LSV signals were measured in 0.1 M Tris-HCl (pH 7.4) at a scanning rate of 50 mV/s.

Optimization of Experimental Conditions for BFC Cathode. To ensure high sensitivity of the as-proposed biosensing strategy and the encapsulation efficiency of csDNA gatekeeper, a serial of experimental conditions were optimized for CV measurements including the bio-gate csDNA concentration, the hybridization reaction time between the target miRNA and the csDNA-capped PMSN, and $[Fe(CN)_6]^{3-}$ concentration incubated with PMSN. As shown in Figure S2A, the cathodic current increased with the increase of csDNA concentration, until it leveled off when the concentration was up to 1.0 nM. It implied that the adsorption between PMSN and csDNA had reached the saturation point, and it could be washed off even if more csDNA added. Thus, 1.0 nM

was chosen as the optimal value. Meanwhile, the time of $[Fe(CN)_6]^{3-}$ release also directly affected the cathodic current signal. In our strategy, because the DNA hybridization reaction and the release of $[Fe(CN)_6]^{3-}$ from the pores were implemented simultaneously, the DNA hybridization reaction also could represent the released circumstances. As shown in Figure S2B, the maximum current appeared at 2 h, which barely changed with prolonging the hybridization time. Hence, 2 h was chosen as the optimum hybridization time`. In addition, the effect of the amount of the entrapped $[Fe(CN)_6]^{3-}$ on the current response was investigated, since the electrochemical signal mainly originated from the electron acceptors. As shown in Figure S2C, the current positively increased initially with the $[Fe(CN)_6]^{3-}$ concentration, and then it reached a plateau when the concentration was up to 100 mM. Thus, 100 mM was chosen as the optimal $[Fe(CN)_6]^{3-}$ concentration.

Fabrication and Characterization of BFC Anode. As the electron generator, the anode was another essential component to ensure the best performance of BFCs. To realize the efficient contact between the enzyme and the indium tin oxide (ITO) substrate, CNT/AuNPs were used as the excellent immobilization matrixes because of their good biocompatibility, high electrical conductivity and chemical stability. Furthermore, the carboxyl-functionalized AuNPs could bond the GOx enzyme molecules through a condensation reaction between the amino groups in enzyme structure and the carboxyl groups on the Au NPs.[5] TEM image of the CNT/AuNPs showed that uniform AuNPs were evenly decorated onto the surface of CNT (Figure 3A), which is in favour of enzymes load. The assembly process of the anode was further confirmed by electrochemical impedance spectroscopy (EIS) measurements. As shown in Figure 3B, compared to the electron-transfer resistance (R_{et}) of the bare ITO (50 Ω, curve a), a smaller R_{et} value (12 Ω, curve b) was obtained for the CNT/AuNPs/ITO electrode, which indicated that CNT/AuNPs enhanced the electron transfer rate. When the electrode was further functionalized with GOx, the resultant GOx/CNT/AuNPs/ITO electrode showed an elevated R_{et} (111 Ω, curve c) due to the fact that the steric hindrance of the enzyme could prevent the redox probes from approaching the electrode surface. Moreover, CVs of the anode without or with 5 mM glucose were carried out to verify the effective oxidation of glucose. In the presence of glucose, both the CV and LSV curves shifted upward compared to their initial values (Figure 3C and 3D), which demonstrated that the anode was sensitive to glucose, in accordance with the mechanism of the O_2-mediated GOx for glucose

oxidation.[49-52] Therefore, excellent catalytic activity of the anode was realized, ensuring the successful construction of the anode used in the self-powered biosensor.

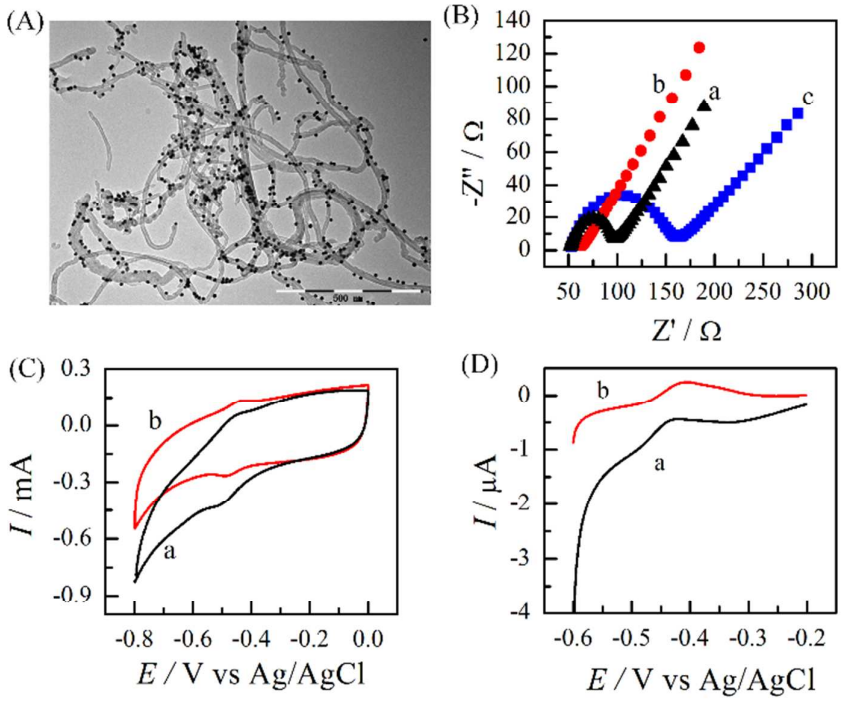

Figure 3. (A) TEM image of the CNT/AuNPs; (B) EIS curves of the bare ITO electrode (a), the CNT/AuNPs/ITO electrode (b), the GOx/CNT/AuNPs/ITO anode (c); (C) CVs of the GOx/CNT/AuNPs/ITO anode in Tris-HCl (pH=7.4) without (a) or with (b) 5 mM glucose, υ = 50 mV/s. (D) LSV of the GOx/CNT/AuNPs/ITO anode in Tris-HCl (pH=7.4) without (a) or with (b) 5 mM glucose, υ = 5 mV/s.

Homogeneous BFC-Based Self-Powered Biosensing of miRNA. Under the optimal conditions, the performance of the as-proposed biosensor for miRNA assay was investigated. As depicted in Figure 4A, in the absence of miRNA-21, the E^{OCV} of the BFC sensor was only 0.42 V (curve a), ascribing to the fact that most of the electron acceptor $[Fe(CN)_6]^{3-}$ was sealed in the porous PMSN and could not gain the electrons generated by the anode. Whereas, in the presence of miRNA-21, the csDNAs were liberated from the surface of PMSN, and then the bio-gate was opened, thus a relatively larger E^{OCV} was observed (curves b to i), which strongly confirmed the feasibility of miRNA-21 induced strategy, and thus homogeneous electrochemical response at the cathode was indeed realized. Moreover, just as expected, the E^{OCV} gradually increased with the elevated miRNA-21 concentration ranging from 0.01 to 1000 fM (Figure 4B). The calibration curve

displayed a linear relationship between E^{OCV} and the miRNA-21 concentration (c), with a linear equation of E^{OCV}=0.511+0.027*logc* and the coefficient of determination (R^2) of 0.9946. The limit of detection (LOD) for miRNA-21 assay was down to 2.7 aM (S/N=3) due to the ingenious design of "signal-on" homogeneous biosensors, which is much lower than those of reported methods (Table S2). Therefore, our homogeneous self-powered biosensor not only provides an integrative and effective strategy to construct easy-to-use bioassays, but also exhibits the features of wider dynamic concentration response range and higher sensitivity for miRNA detection.

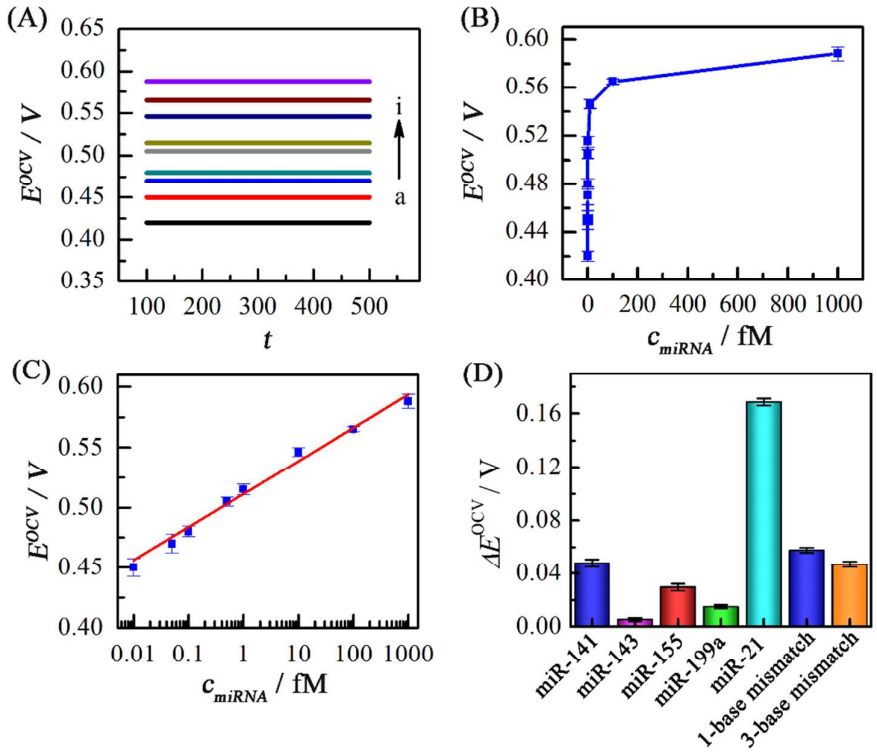

Figure 4. (A) E^{OCV} of the proposed biosensor in the presence of miRNA-21 with different concentrations (from a to i: 0, 0.01, 0.05, 0.1, 0.5, 1, 10, 100, 1000 fM); (B) The curve of E^{OCV} values versus miRNA-21 concentration; (C) The linear relationship between E^{OCV} and the logarithm of miRNA-21 concentration from 0.01 to 1000 fM; (D) Comparison of ΔE^{OCV} for the biosensing platform in the presence of miRNA-21 and four interfering miRNAs and the base mismatched strands, respectively, with the same concentration of 1.0 pM; $\Delta E^{OCV} = E^{OCV} - E_0{}^{OCV}$, in which $E_0{}^{OCV}$ was the blank signal of BFC in the absence of miRNAs. Error bars represent the standard deviation of an average value from independent measurements of three biosensors.

Selectivity and Reproducibility. To evaluate the selectivity of the proposed BFC sensor, four other miRNAs, *i.e.* miRNA-141, miRNA-143, miRNA-155 and miRNA-199a, and the base mismatched strands, with the same concentration as that of miRNA-21, were selected as the interfering miRNAs. Figure 4D shows that in the presence of whether the interfering miRNAs or the mismatched strands, the ΔE^{OCV} values were much lower than that of the target miRNAs due to the high specificity of base pairing reaction, which demonstrated that the proposed biosensor had good selectivity for discriminating the target miRNA. Moreover, the reproducibility of the biosensor is also a key issue, which was investigated by repeating the measurements 12 times within a week. The relative standard deviation (*RSD*) was determined to be less than 8.0% for the determination of 1.0 pM miRNA in a week using biosensors that were freshly fabricated, indicating an acceptable reproducibility of the as-proposed strategy.

miRNA Detection in Serum Samples. To validate the application potential of the proposed self-powered biosensing platform, the human serum samples extracted from cancer patients, in which miRNA-21 is overexpressed, were measured. As the results (Table S3) demonstrated, our method would be competent for directly determining the miRNA-21 in serum samples, needing no separation or enrichment. Furthermore, standard addition method was further used to evaluate the reliability of the as-prepared biosensor. The satisfactory RSD (3.37%~4.70%) and recovery results (95.5%~110%) suggested that the as-proposed self-powered biosensor has great promise to be applied for miRNA bioassay in clinical diagnosis. To further extend the practical application of the as-proposed biosensing system, there is still room to improve its analytical performance, including better stability of the BFC, more excellent performance of anode for higher sensitivity, more robust anti-interference property for better specificity and more miniature devices for portable and/or on-site bioassay.

CONCLUSION

In summary, we have developed, for the first time, an efficient and easy-to-use biosensors for ultrasensitive miRNA bioassay *via* the integration of homogeneous strategy and BFC-based self-powered biosensing. Encouragingly, the as-proposed biosensor possesses the merits of wider dynamic concentration response range and higher sensitivity for miRNA detection, which can be

ascribed to the ingenious design of the target-induced $[Fe(CN)_6]^{3-}$ release to enable the "signal-on" homogeneous electrochemical assay of miRNA. Therefore, this versatile homogeneous self-powered biosensing strategy may become an alternative method to realize simple, rapid, reliable and ultrasensitive bioassays and it has great potential to be applied in miRNA-related clinical diagnostics and biochemical research.

ASSOCIATED CONTENT

Supporting Information

Additional information as noted in the main text. Optimization of experimental conditions for BFC cathode; Sequences of the oligonucleotides used in the experiments; Comparison of analytical performance for miRNA detection by our method and those reported in literature; Measurement of miRNA-21 in human serum samples

AUTHOR INFORMATION

Corresponding Author

*E-mails: lifeng@qust.edu.cn (F. Li)

Tel/Fax: (86) 532-86080855

Notes

The authors declare no competing financial interest.

ACKNOWLEDGMENT

We gratefully appreciate the financial support from the National Natural Science Foundation of China (21605092, 21675095, and 21575074), the Natural Science Foundation of Shandong Province, China (ZR2016BQ08), the Research Foundation for Distinguished Scholars of Qingdao Agricultural University (663-1117002), and the Special Foundation for Taishan Scholar of Shandong Province (No. ts201511052).

REFERENCES

1. Gao, F.; Viry, L.; Maugey, M.; Poulin, P.; Mano, N., Engineering Hybrid Nanotube Wires for High-Power Biofuel Cells. *Nat. Commun.* **2010**, *1*, 2.
2. Cosnier, S.; J. Gross, A.; Le Goff, A.; Holzinger, M., Recent Advances on Enzymatic Glucose/Oxygen and Hydrogen/Oxygen Biofuel Cells: Achievements and Limitations. *J. Power Sources* **2016**, *325*, 252-263.
3. Stolarczyk, K.; Kizling, M.; Majdecka, D.; Żelechowska, K.; Biernat, J. F.; Rogalski, J.; Bilewicz,

R., Biobatteries and Biofuel Cells with Biphenylated Carbon Nanotubes. *J. Power Sources* **2014**, *249*, 263-269.

4. Miyake, T.; Yoshino, S.; Yamada, T.; Hata, K.; Nishizawa, M., Self-Regulating Enzyme-Nanotube Ensemble Films and Their Application as Flexible Electrodes for Biofuel Cells. *J. Am. Chem. Soc.* **2011**, *133*, 5129-5134.
5. Chen, Y.; Gai, P. P.; Zhang, J. R.; Zhu, J. J., Design of an Enzymatic Biofuel Cell with Large Power Output. *J. Mater. Chem. A* **2015**, *3*, 11511-11516.
6. Katz, E.; Bückmann, A. F.; Willner, I., Self-Powered Enzyme-Based Biosensors. *J. Am. Chem. Soc.* **2001**, *123*, 10752-10753.
7. Arechederra, R.; Minteer, S., Self-Powered Sensors. *Anal. Bioanal. Chem* **2011**, *400*, 1605-1611.
8. Wen, D.; Deng, L.; Guo, S.; Dong, S., Self-Powered Sensor for Trace Hg^{2+} Detection. *Anal. Chem.* **2011**, *83*, 3968-3972.
9. Rasmussen, M.; Minteer, S. D., Self-Powered Herbicide Biosensor Utilizing Thylakoid Membranes. *Anal. Methods* **2013**, *5*, 1140-1144.
10. Hou, C.; Fan, S.; Lang, Q.; Liu, A., Biofuel Cell Based Self-Powered Sensing Platform for L-Cysteine Detection. *Anal. Chem.* **2015**, *87*, 3382-3387.
11. Zhou, M.; Du, Y.; Chen, C.; Li, B.; Wen, D.; Dong, S.; Wang, E., Aptamer-Controlled Biofuel Cells in Logic Systems and Used as Self-Powered and Intelligent Logic Aptasensors. *J. Am. Chem. Soc.* **2010**, *132*, 2172-2174.
12. Lin, Z. H.; Cheng, G.; Wu, W. Z.; Pradel, K. C.; Wang, Z. L., Dual-Mode Triboelectric Nanogenerator for Harvesting Water Energy and as a Self-Powered Ethanol Nanosensor. *ACS Nano* **2014**, *8*, 6440-6448.
13. Jung, Y. K.; Kim, K. N.; Baik, J. M.; Kim, B. S., Self-Powered Triboelectric Aptasensor for Label-Free Highly Specific Thrombin Detection. *Nano Energy* **2016**, *30*, 77-83.
14. Cheng, J.; Han, Y.; Deng, L.; Guo, S., Carbon Nanotube–Bilirubin Oxidase Bioconjugate as a New Biofuel Cell Label for Self-Powered Immunosensor. *Anal. Chem.* **2014**, *86*, 11782-11788.
15. Wang, Y.; Ge, L.; Wang, P.; Yan, M.; Yu, J.; Ge, S., A Three-Dimensional Origami-Based Immuno-Biofuel Cell for Self-Powered, Low-Cost, and Sensitive Point-of-Care Testing. *Chem. Commun.* **2014**, *50*, 1947-1949.
16. Gai, P. P.; Song, R. B.; Zhu, C.; Ji, Y. S.; Wang, W. J.; Zhang, J. R.; Zhu, J. J., Ultrasensitive Self-Powered Cytosensors Based on Exogenous Redox-Free Enzyme Biofuel Cells as Point-of-Care Tools for Early Cancer Diagnosis. *Chem. Commun.* **2015**, *51*, 16763-16766.
17. Gai, P. P.; Ji, Y. S.; Wang, W. J.; Song, R. B.; Zhu, C.; Chen, Y.; Zhang, J. R.; Zhu, J. J., Ultrasensitive Self-Powered Cytosensor. *Nano Energy* **2016**, *19*, 541-549.
18. Gamella, M.; Guz, N.; Mailloux, S.; Pingarrón, J. M.; Katz, E., Activation of a Biocatalytic Electrode by Removing Glucose Oxidase from the Surface-Application to Signal Triggered Drug Release. *ACS Appl. Mater. Interfaces* **2014**, *6*, 13349-13354.
19. Zhou, M.; Zhou, N.; Kuralay, F.; Windmiller, J. R.; Parkhomovsky, S.; Valdés−Ramírez, G.; Katz, E.; Wang, J., A Self−Powered "Sense−Act−Treat" System That Is Based on a Biofuel Cell and Controlled by Boolean Logic. *Angew. Chem. Int. Ed.* **2012**, *51*, 2686-2689.
20. Gamella, M.; Guz, N.; Mailloux, S.; Pingarrón, J. M.; Katz, E., Antibacterial Drug Release Electrochemically Stimulated by the Presence of Bacterial Cells - Theranostic Approach. *Electroanalysis* **2014**, *26*, 2552-2557.
21. Zhou, M.; Wang, J., Biofuel Cells for Self-Powered Electrochemical Biosensing and Logic

Biosensing: A Review. *Electroanalysis* **2012**, *24*, 197-209.

22. Zhou, M., Recent Progress on the Development of Biofuel Cells for Self-Powered Electrochemical Biosensing and Logic Biosensing: A Review. *Electroanalysis* **2015**, *27*, 1786-1810.
23. Katz, E.; Privman, V., Enzyme-Based Logic Systems for Information Processing. *Chem. Soc. Rev.* **2010**, *39*, 1835-1857.
24. Zhu, Z.; Tam, T. K.; Sun, F.; You, C.; Zhang, Y.-H. P., A High-Energy-Density Sugar Biobattery Based on a Synthetic Enzymatic Pathway. *Nat. Commun.* **2014**, *5*, 3026.
25. Rowe, A. A.; Chuh, K. N.; Lubin, A. A.; Miller, E. A.; Cook, B.; Hollis, D.; Plaxco, K. W., Electrochemical Biosensors Employing an Internal Electrode Attachment Site and Achieving Reversible, High Gain Detection of Specific Nucleic Acid Sequences. *Anal. Chem.* **2011**, *83*, 9462-9466.
26. Acunzo, M.; Romano, G.; Wernicke, D.; Croce, C. M., Microrna and Cancer – a Brief Overview. *Adv. Biol. Regul.* **2015**, *57*, 1-9.
27. Válóczi, A.; Hornyik, C.; Varga, N.; Burgyán, J.; Kauppinen, S.; Havelda, Z., Sensitive and Specific Detection of Micrornas by Northern Blot Analysis Using Lna-Modified Oligonucleotide Probes. *Nucleic Acids Res.* **2004**, *32*, e175.
28. Clancy, E.; Burke, M.; Arabkari, V.; Barry, T.; Kelly, H.; Dwyer, R. M.; Kerin, M. J.; Smith, T. J., Amplification-Free Detection of Micrornas via a Rapid Microarray-Based Sandwich Assay. *Anal Bioanal Chem* **2017**, *409*, 3497-3505.
29. Pritchard, C. C.; Cheng, H. H.; Tewari, M., Microrna Profiling: Approaches and Considerations. *Nat. Rev. Genet.* **2012**, *13*, 358-369.
30. Zhou, Y.; Zhang, J.; Zhao, L.; Li, Y.; Chen, H.; Li, S.; Cheng, Y., Visual Detection of Multiplex Micrornas Using Cationic Conjugated Polymer Materials. *ACS Appl. Mater. Interfaces* **2016**, *8*, 1520-1526.
31. Li, W.; Hou, T.; Wu, M.; Li, F., Label-Free Fluorescence Strategy for Sensitive MicroRNA Detection Based on Isothermal Exponential Amplification and Graphene Oxide. *Talanta* **2016**, *148*, 116-121.
32. Li, L.; Feng, J.; Liu, H.; Li, Q.; Tong, L.; Tang, B., Two-Color Imaging of MicroRNA with Enzyme-Free Signal Amplification via Hybridization Chain Reactions in Living Cells. *Chem. Sci.* **2016**, *7*, 1940-1945.
33. Xu, Q.; Ma, F.; Huang, S. Q.; Tang, B.; Zhang, C. Y., Nucleic Acid Amplification-Free Bioluminescent Detection of MicroRNAs with High Sensitivity and Accuracy Based on Controlled Target Degradation. *Anal. Chem.* **2017**, *89*, 7077-7083.
34. Ma, F.; Liu, M.; Tang, B.; Zhang, C. Y., Sensitive Quantification of MicroRNAs by Isothermal Helicase-Dependent Amplification. *Anal. Chem.* **2017**, *89*, 6182-6187.
35. Zhang, H.; Liu, Y.; Gao, J.; Zhen, J., A Sensitive Sers Detection of miRNA Using a Label-Free Multifunctional Probe. *Chem. Commun.* **2015**, *51*, 16836-16839.
36. Deng, R.; Tang, L.; Tian, Q.; Wang, Y.; Lin, L.; Li, J., Toehold-Initiated Rolling Circle Amplification for Visualizing Individual MicroRNAs in Situ in Single Cells. *Angew. Chem. Int. Ed.* **2014**, *53*, 2389-2393.
37. Zhang, P. H.; He, Z. M.; Wang, C.; Chen, J. N.; Zhao, J. J.; Zhu, X. N.; Li, C. Z.; Min, Q. H.; Zhu, J. J., In Situ Amplification of Intracellular MicroRNA with Mnazyme Nanodevices for Multiplexed Imaging, Logic Operation, and Controlled Drug Release. *ACS Nano* **2015**, *9*,

789-798.

38. Lu, W.; Chen, Y.; Liu, Z.; Tang, W.; Feng, Q.; Sun, J.; Jiang, X., Quantitative Detection of MicroRNA in One Step Via Next Generation Magnetic Relaxation Switch Sensing. *ACS Nano* **2016**, *10*, 6685-6692.
39. Yuan, Y.-H.; Wu, Y.-D.; Chi, B.-Z.; Wen, S.-H.; Liang, R.-P.; Qiu, J.-D., Simultaneously Electrochemical Detection of MicroRNAs Based on Multifunctional Magnetic Nanoparticles Probe Coupling with Hybridization Chain Reaction. *Biosens. Bioelectron.* **2017**, *97*, 325-331.
40. Rafiee-Pour, H. A.; Behpour, M.; Keshavarz, M., A Novel Label-Free Electrochemical miRNA Biosensor Using Methylene Blue as Redox Indicator: Application to Breast Cancer Biomarker miRNA-21. *Biosens. Bioelectron.* **2016**, *77*, 202-207.
41. Chen, A.; Ma, S.; Zhuo, Y.; Chai, Y.; Yuan, R., In Situ Electrochemical Generation of Electrochemiluminescent Silver Naonoclusters on Target-Cycling Synchronized Rolling Circle Amplification Platform for MicroRNA Detection. *Anal. Chem.* **2016**, *88*, 3203-3210.
42. Wang, L. L.; Shao, H. H.; Wang, W. J.; Zhang, J. R.; Zhu, J. J., Nitrogen-Doped Hollow Carbon Nanospheres for High-Energy-Density Biofuel Cells and Self-Powered Sensing of MicroRNA-21 and MicroRNA-141. *Nano Energy* **2018**, 44, 95-102.
43. Hou, T.; Li, W.; Liu, X.; Li, F., Label-Free and Enzyme-Free Homogeneous Electrochemical Biosensing Strategy Based on Hybridization Chain Reaction: A Facile, Sensitive, and Highly Specific MicroRNA Assay. *Anal. Chem.* **2015**, *87*, 11368-11374.
44. Ge, L.; Wang, W. X.; Li, F., Electro-Grafted Electrode with Graphene-oxide-like DNA Affinity for Ratiometric Homogeneous Electrochemical Biosensing of MicroRNA. *Anal. Chem.* **2017**, *89*, 11560-11567.
45. Gai, P. P.; Gu, C. C.; Li, H. Y.; Sun, X. Z.; Li, F., Ultrasensitive Ratiometric Homogeneous Electrochemical MicroRNA Biosensing via Target-Triggered Ru(III) Release and Redox Recycling. *Anal. Chem.* **2017**, *89*, 12293-12298.
46. Wang, J.; Li, X. L.; Zhang, J. D.; Hao, N.; Xu, J. J.; Chen, H. Y., Integration of DNA Bio-Gates and Duplex-Specific Nuclease Signal Amplification: Towards Electrochemiluminescence Detection of Survivin mRNA. *Chem. Commun.* **2015**, *51*, 11673-11676.
47. Xu, Q.; Cai, W. Y.; Zhu, J. J., Self-Assembly of Horseradish Peroxidase on Biocompatible Gold Nanoparticles-Vaterite Core-Shell Composite and Its Direct Electrochemistry. *Chem. Lett.* **2005**, *34*, 832-833.
48. Gu, C. C.; Gai, P. P.; Hou, T.; Li, H. Y.; Xue, C. H.; Li, F., Enzymatic Fuel Cell-Based Self-Powered Homogeneous Immunosensing Platform via Target-Induced Glucose Release: An Appealing Alternative Strategy for Turn-on Melamine Assay. *ACS Appl. Mater. Interfaces* **2017**, *9*, 35721-35728.
49. Hyun, K. H.; Han, S. W.; Koh, W.-G.; Kwon, Y., Fabrication of Biofuel Cell Containing Enzyme Catalyst Immobilized by Layer-by-Layer Method. *J. Power Sources* **2015**, *286*, 197-203.
50. Wooten, M.; Karra, S.; Zhang, M.; Gorski, W., On the Direct Electron Transfer, Sensing, and Enzyme Activity in the Glucose Oxidase/Carbon Nanotubes System. *Anal. Chem.* **2014**, *86*, 752-757.
51. Christwardana, M.; Kim, K. J.; Kwon, Y., Fabrication of Mediatorless/Membraneless Glucose/Oxygen Based Biofuel Cell Using Biocatalysts Including Glucose Oxidase and Laccase Enzymes. *Sci. Rep.* **2016**, *6*, 30128.
52. Milton, R. D.; Minteer, S. D., Direct Enzymatic Bioelectrocatalysis: Differentiating between Myth

and Reality. *J. R. Soc. Interface* **2017**, *14*, 20170253.

For TOC only

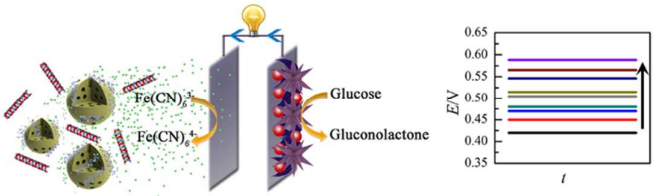
Fe(CN)6 3-
Fe(CN)6 4-
Glucose
Gluconolactone
0.65
0.60
0.55
0.50
0.45
0.40
0.35
E/V
t